



Design of thermally coupled reactive distillation schemes for triethyl citrate production using economic and controllability criteria



Miguel A. Santaella^a, Luis E. Jiménez^a, Alvaro Orjuela^{a,*}, Juan Gabriel Segovia-Hernández^b

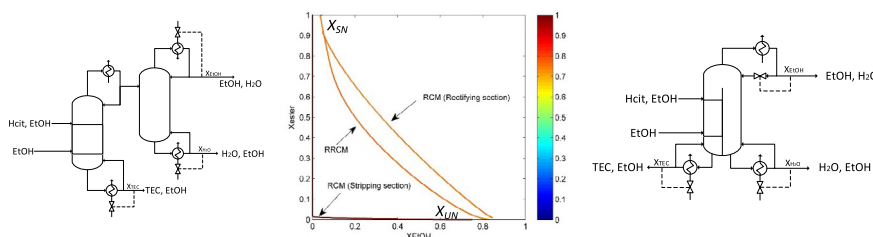
^a Universidad Nacional de Colombia, Ciudad Universitaria, Department of Chemical and environmental Engineering, Bogotá DC, Colombia

^b Facultad de Química, Universidad de Guanajuato, Noria Alta s/n, Guanajuato, Gto. 36050, Mexico

HIGHLIGHTS

- Conceptual design of a triethyl citrate process was carried out.
- Reactive residue curve maps used for conceptual design of a multi-reaction system.
- Reactive dividing wall column used as intensification alternative.
- Optimization including controllability at early stages of conceptual design.
- Large energy savings using dividing wall columns with acceptable controllability.

GRAPHICAL ABSTRACT



ARTICLE INFO

Article history:

Received 24 March 2017

Received in revised form 22 June 2017

Accepted 5 July 2017

Available online 6 July 2017

Keywords:

Triethyl citrate
Reactive distillation
Dividing wall column
Controllability
Optimization

ABSTRACT

This work describes a systematic process design for triethyl citrate production by direct esterification of citric acid with ethanol via simultaneous reaction-separation technologies. The design methodology includes simultaneous optimization of controllability and profitability criteria. With a novel approach, the conceptual feasibility analysis of the intensified processes was carried out by extending the reactive residue curve maps (RRCM) to mixtures with six components by implementing a substitution degree parameter. The RRCM have been also extended to the conceptual design of dividing wall columns. The configuration of both, traditional and dividing wall reactive distillation columns, were obtained from the conceptual analysis. The processes were simulated using experimentally validated models, and further optimized using a nature inspired multi-objective algorithm. A triethyl citrate production capacity of 10 kTon/yr was used as process specification. Final designs evidenced citric acid conversions above 99.9%, energy consumption from 3–5 MJ/kg, and a TEC production costs of c.a 1.5 USD/kg. Controllability assessment was performed by evaluating the condition number of the proposed operating schemes. Pareto diagrams indicate that the minimization of total annual costs and controllability are conflicting goals in both production schemes. Nevertheless, both alternatives withstand large perturbations over the main process variables. The reactive dividing wall column scheme results in large energy and cost savings over a traditional reactive distillation process.

© 2017 Elsevier B.V. All rights reserved.

1. Introduction

Over the last decade, bioderived molecules have increased their market share in the plasticizers sector due to the increasing concerns on the toxicity, biodegradability and sustainability of traditional petroleum based plasticizers [1]. Despite the fact that

* Corresponding author.

E-mail address: aoorjuel@unal.edu.co (A. Orjuela).

Nomenclature

List of Symbols and Abbreviations

a_i	activity of component i in the liquid phase	RD	reactive distillation
B_f	molar flow of bottoms product	RDWC	reactive dividing wall column
CA	citric acid	RRCM	reactive residue curve map
CN	condition number	SD	substitution degree
COF	controllability objective function	SDV	singular value decomposition
D_f	molar flow of distillate	t	time, s
DEC	diethyl citrate	T	temperature
DEE	diethyl ether	TAC	total annual cost, \$/yr
D_e	equivalent diameter for RDWC	TEC	triethyl citrate
D_{prefac}	prefractionator column diameter	V	vapor molar flow, mol/s
D_{main}	main column diameter	w_{cat}	catalyst loading, kg_{cat}/kg_{sol}
E_A	activation energy, kJ/kmol	X_{ester}	total mole fraction of citric esters in the liquid mixture
EtOH	ethanol	X_{EtOH}	reduced concentration of ethanol in the liquid mixture
H	molar holdup of residual liquid, mol	x_i	liquid mole fraction of component i
$K_{cat,n}$	kinetic constant for catalytic reaction n , $kg_{sol}/kg_{cat} s^{-1}$	X_{SN}	stable node of a residue curve map
$K_{cat,n}^0$	pre-exponential factor for catalytic reaction n , $kg_{sol}/kg_{cat} s^{-1}$	X_{UN}	unstable node of a residue curve map
$K_{self,n}$	kinetic constant for autocatalytic reaction n , $kg_{sol}/kg_{cat} s^{-1}$	y_i	vapor mole fraction of component i
$K_{self,n}^0$	pre-exponential factor for autocatalytic reaction n , $kg_{sol}/kg_{cat} s^{-1}$	Y_{ester}	reduced concentration of citric esters in the liquid mixture
K_n	equilibrium constant of reaction n		
M_f	molar holdup of stage f	Greek Letters	
MEC	monoethyl citrate	ΔS_i	supply imbalance of component i due to a given disturbance
MNG	maximum number of generations	ξ	forward dimensionless integration variable
MODE	multi-objective differential evolution	σ	backward dimensionless integration variable
NP	population size	k_{pq}	gain of controlled variable p when manipulated variable q is disturbed
Pc	crossover probability	$v_{i,j}$	stoichiometric coefficient of component i in reaction j
Pm	mutation probability	$v_{T,j}$	sum of the stoichiometric coefficients in reaction j .
r_j	rate of reaction j , s^{-1}	τ	residence time
RCM	non-reactive residue curve trajectory	τ_q	characteristic time

petroleum-based phthalate plasticizers still dominate the current global market (above 80% of world production), it is expected that biobased substitutes will represent nearly 30% of the total market in coming years [2–5]. In some niche applications such as the fabrication of medical devices, toys, food/feed packing, pharmaceuticals and cosmetics; non-phthalate alternatives are preferred for polymers plasticization. Nevertheless, not all biobased plasticizers have shown better technical performance than the widely used phthalic acid esters. Among various environmentally friendly alternatives, triethyl citrate (TEC) (with or without acetylation) is a well-known phthalate substitute in different applications. In addition to its good plasticizing properties, TEC is generally recognized as safe (GRAS) [6] which make it suitable for sensitive products.

In spite of the TEC benefits from a social and environmental standpoint, its sustainability as a phthalate substitute is still questioned due to the high costs [7]. Factors increasing TEC production costs include: the use of batch instead of continuous processing; the higher prices of the biobased feedstocks (compared with petroleum derived); the need for alcohol excess to dissolve citric acid and to overcome chemical equilibrium limitations; and the large energy consumption in the separation operations. In this direction, there is need for developing enhanced TEC production processes, and to screen them at the early stages of the design to establish their technical and economic feasibility before up-scaling [8]. Some attempts to reduce TEC production costs through process intensification have been recently reported [9–14]. To reduce the excess of ethanol (EtOH), continual displacement of the esterification equilibrium has been achieved via reactive distillation (RD) [10].

Further improvements by using a RD column with side reactors have also been considered [15]. Additionally, energy saving technologies such as heat integration and thermal coupling have been proposed for TEC RD processes [16].

In recent years, the use of side rectifiers, side strippers, Petlyuk columns, and reactive dividing wall columns (RDWC), as thermally integrated sequences, have shown benefits in terms of capital cost reduction and energy savings in different reactive systems [15–17]. However, a high degree of integration makes process design and optimization a non-trivial task due to the increase in the number of degrees of freedom, and the complex behavior of the intensified units [18]. Although better control characteristics have been observed in some thermally coupled configurations over the traditional ones [19], such verifications are seldom performed due to the complexity of the resulting dynamic mathematical model. Therefore, annual costs and energy consumption are often selected as objective functions during process synthesis and optimization, while controllability is evaluated at a later stage.

To include controllability within the preliminary stages of the design process, recent reports described how the dynamic behavior of distillation columns for multicomponent mixtures can be approximately quantified through the evaluation of steady state simulations assuming first order responses [20]. The methodology consists on performing small perturbations in the manipulated variables of an open loop steady-state simulation, and extracting the gain matrix from the differences observed in the controlled variables. As a result, the time constant from the observed changes in molar holdup and molar flow rate of a key component are

obtained. This, allows a readily evaluation of controllability and its subsequent inclusion as a part of the objective function in the preliminary design stages [21].

In this regard, this work describes the extension of the proposed methodology to a RD sequences and furthermore, to a reactive dividing wall column (RDWC), for the specific case of TEC production. Both operating schemes were simulated based upon experimentally validated models. After completing the steady state simulations, the total annual costs were calculated based upon Guthrie's correlations for the bare modules, and the updated prices for raw materials and catalytic packings. Subsequently, disturbances over the control variables were done to approximate the dynamic behavior to a first order response, obtaining the transfer matrix. Then, the matrix was used to calculate the controllability via condition number calculation. Finally, a multi-objective optimization for each schemes was carried out using a nature-inspired algorithms, taking into account total annual costs and controllability as objective functions.

2. Process design basics

2.1. Kinetic models and thermodynamics

The esterification of citric acid (CA) with EtOH to produce TEC involves three consecutive reversible reactions, with monoethyl citrate (MEC) and diethyl citrate (DEC) as intermediate products, and water as the main byproduct (Fig. 1). An additional side reaction under acidic conditions and high temperatures might occur when ethanol dehydrates to diethyl ether (DEE).

Although the reaction between CA and EtOH has been widely studied, there are few kinetic models available in the open literature. A recent study of CA esterification with EtOH using Amberlyst 15 as catalyst reported a kinetic model that includes an autocatalytic contribution. The kinetic equations are presented in Eqs.

(1)(5) and the corresponding parameters are summarized in Table 1. As previously reported, the conversion of the reaction is limited by chemical equilibrium, and consequently, the continual removal of water is required to promote a higher degree of substitution. This task can be accomplished by coupling reaction and distillation within a reactive distillation (RD) column [10].

$$-\frac{dx_{CA}}{dt} = (w_{cat}K_{cat1} + x_{acid}K_{self1}) \left(a_{CA}a_{EtOH} - \frac{a_{H_2O}a_{MEC}}{K_1} \right) \quad (1)$$

$$-\frac{dx_{MEC}}{dt} = (w_{cat}K_{cat2} + x_{acid}K_{self2}) \left(a_{MEC}a_{EtOH} - \frac{a_{H_2O}a_{DEC}}{K_2} \right) \quad (2)$$

$$-\frac{dx_{DEC}}{dt} = (w_{cat}K_{cat3} + x_{acid}K_{self3}) \left(a_{DEC}a_{EtOH} - \frac{a_{H_2O}a_{TEC}}{K_3} \right) \quad (3)$$

$$-\frac{dx_{DEE}}{dt} = -w_{cat}K_{cat,4} \quad (4)$$

$$x_{acid} = \left(x_{CA} + \frac{2}{3}x_{MEC} + \frac{1}{3}x_{DEC} \right) \quad (5)$$

$$K_{cat,i} = K_{cat,i}^0 \quad (6)$$

$$K_{self,i} = K_{self,i}^0 \quad (7)$$

Regarding phase equilibria, the reactive system exhibits highly non-ideal behavior with immiscibility in the liquid phase, a homogeneous azeotrope, and partial dissociation of the acid components in aqueous solutions. In a previous work, Kolah et al. [9] evaluated TEC-EtOH and TEC-H₂O binary VLE data, and also used UNIFAC predictions to regress a set parameters for the UNIQUAC equation. While liquid phase was assumed non-ideal, Ideal gas phase was used during parameter fitting. In this work, Gani's method was used to estimate MEC and DEC boiling points, and such

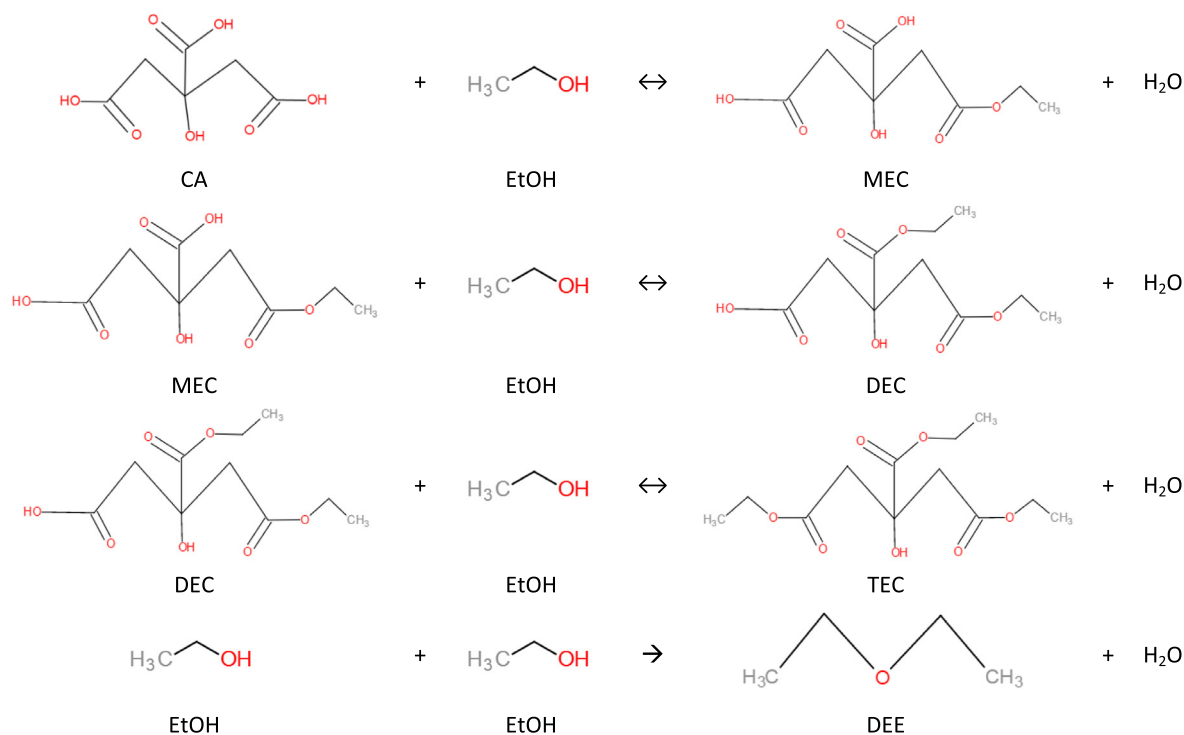


Fig. 1. Reaction scheme in esterification of citric acid (CA) with ethanol (EtOH) to produce triethyl citrate (TEC). Monoethyl citrate (MEC) and Diethyl Citrate (DEC) are intermediate esters, and water (H₂O) is a byproduct. Diethyl ether (DEE) is a side product of ethanol decomposition.

Table 1
Kinetic Model parameters for self-catalyzed and resin-catalyzed reactions [9]

Parameter	Units	Value
$K_{cat,1}^o$	$kg_{sol}/(kg_{cat} \cdot s)$	3.34×10^8
$K_{cat,2}^o$		1.87×10^9
$K_{cat,3}^o$		1.99×10^7
$K_{cat,4}^o$		3.35×10^8
$E_{A,cat,1}$	$kJ/kmol$	76900
$E_{A,cat,2}$		83100
$E_{A,cat,3}$		73200
$E_{A,cat,4}$		102000
$K_{self,1}^o$	$1/s$	3.34×10^8
$K_{self,2}^o$		1.87×10^9
$K_{self,3}^o$		1.99×10^7
$E_{A,self,1}$	$kJ/kmol$	76900
$E_{A,self,2}$		83100
$E_{A,self,3}$		73200
K_1		6.35
K_2		2.72
K_3		3.78

information was later used to regress Antoine parameters for intermediate species. The complete set of Antoine parameters is presented in Table S.1 in the Supporting material. Additionally, Berdugo *et al.* [22] obtained experimental DEC-EtOH and DEC-H₂O binary VLE data that validated previous predictions. The list of UNIQUAC parameters for the calculation of liquid phase activities are listed in Table S.2 in the Supporting material. In this work, vapor phase was also assumed ideal.

2.2. Conceptual design of reactive distillation

Despite the idea of implementing a CA esterification via RD might seem straightforward [10], some particularities of this reactive system have to be considered when modeling the operation. As CA is solid, there must be a minimum amount of EtOH to guarantee complete solubility of reactants and a good compatibility with the catalyst (CA solubility in EtOH is 5–8% mol at 303 K, [23]). The required EtOH excess for complete miscibility of reactants also contributes to improve the reaction conversion. Nevertheless, it involves large energy consumption for EtOH recovery and recycle.

An important decisions to make prior to the feasibility analysis is defining the operating pressure of the RD system because it determines the operating temperatures within the column. In this particular reactive system, there is a limit in the operating temperatures because of CA thermal instability (decomposing above 413 K [9,24,25]); and the ion exchange catalysts degradation (around 403 K). Also, side reactions such as ethanol dehydration, oxidations, and citrates decompositions occur at high temperatures. Once those considerations are contemplated, the conceptual design of RD schemes can be carried out by analyzing the behavior of reactive residue curve maps (RRCM). In this case, not only chemical equilibrium but reaction kinetics must be taken into account. The procedure for obtaining Eqs. (5) and (6) that describes the construction of RRCM under kinetic regime is presented elsewhere [26].

$$\frac{dx_i}{d\xi} = [x_i - y_i] + \frac{H}{V} \sum_{j=1}^c \{r_j(v_{i,j} - x_i v_{T,j})\} \quad (8)$$

$$\frac{dx_i}{d\sigma} = -[x_i - y_i] - \frac{H}{V} \sum_{j=1}^c \{r_j(v_{i,j} - x_i v_{T,j})\} \quad (9)$$

Here x_i and y_i correspond to the molar fraction of component i in the liquid and vapor phase respectively. r_j is the rate of reaction j , H is

the molar holdup of residual liquid, V is the vapor molar flow, ξ and σ are the forward and backward dimensionless integration variables respectively, $v_{i,j}$ is the stoichiometric coefficient of component i in reaction j , and $v_{T,j}$ is the sum of the stoichiometric coefficients in reaction j .

The generation of reactive residue curves can be done by integrating Eq. (8) from $\xi = 0$ to $\xi = \infty$, and Eq. (9) from $\sigma = -\infty$ to $\sigma = 0$. The initial composition ($x_{o,i}$) for the integration can be selected either as a mixture of reactants only, or even as any other random composition. However, to generate $x_{o,i}$ by a more meaningful and systematic way, it was obtained from the integration of a batch pre-reactor (Eqs. (10) and (11)) with different residence times (τ). This would also represent a potential feed stream composition obtained from a pre-reactor upstream the RD column.

$$x_{o,i} = x_{p,i} + \int_0^\tau \frac{dx_i}{dt} dt \quad (10)$$

$$\frac{dx_i}{dt} = \sum_{j=1}^c \{r_j(v_{i,j} - x_i v_{T,j})\} \quad (11)$$

As there are seven components in the reactive mixture, plotting a classic two dimensional RRCM diagram is not possible. Therefore, to overcome this limitation, three considerations were implemented. First, the production of undesired diethyl ether from Eq. (4) was not taken into account for the construction of residue curves. Second, all citric esters were lumped as a single pseudo-ester component of concentration x_{ester} , according to Eqs. (12) and (13). Finally, a reduced concentration scale [27] calculated by Eqs. (14) and (15) was used to plot a pseudo-quaternary diagram.

$$x_{ester} = x_{MEC} + x_{DEC} + x_{TEC} \quad (12)$$

$$x_{CA} + x_{EtOH} + x_{H_2O} + x_{ester} = 1 \quad (13)$$

$$x_{EtOH} = x_{EtOH} + x_{CA} \quad (14)$$

$$x_{ester} = x_{ester} + x_{CA} \quad (15)$$

So, with the lumped variables, a pseudo-quaternary RRCM square diagram on transformed coordinates was constructed. For clarity, each side of a pseudo-quaternary diagram plot represents a binary mixture, while the corners correspond to the pure components (or pseudo-components). This is described in Fig. S.1 of the Supporting material and in the following reactive residue curve maps. Easily identified are the “pure” lumped ester node ($x_{ester} = 1$, $x_{EtOH} = 0$) and the pure EtOH node ($x_{ester} = 0$, $x_{EtOH} = 1$). At the bottom-left corner ($x_{ester} = 0$, $x_{EtOH} = 0$) is located the pure water node, while the pure CA is placed at the top-right end ($x_{ester} = 1$, $x_{EtOH} = 1$). In the reduced composition scale, the binary mixtures of EtOH-CA are located at any point in $x_{EtOH} = 1$, and the EtOH-H₂O mixtures are situated at any point in $x_{ester} = 0$.

With this in mind, this diagram will be used from now on to express the relative compositions in a RRCM. Additionally, to quantify the relative content of the different esters (mono-, di- or tri-ester) and CA in the reactive media, the substitution degree concept is here introduced. The substitution degree (SD) was defined as the amount of esterified acid groups in all citrates species over the total amount of esterified and non-esterified acid groups, and it was calculated using in Eq. (16).

$$SD = \frac{x_{MEC} + 2x_{DEC} + 3x_{TEC}}{3x_{AC} + 3x_{MEC} + 3x_{DEC} + 3x_{TEC}} = \frac{\frac{1}{3}x_{MEC} + \frac{2}{3}x_{DEC} + x_{TEC}}{x_{AC} + x_{MEC} + x_{DEC} + x_{TEC}} \quad (16)$$

Theoretical SD values for pure CA, MEC, DEC and TEC are 0, 0.33, 0.67, and 1 respectively; so higher SD values correspond to a higher content of TEC. With this in mind, a color scale based upon the SD

value was used to draw the lines within the RRCM. This color scale provides particular insights on the reaction selectivity, and it might help elucidating the chemical nature of products in the RD system.

Eqs. (5) and (6) were solved for an operating pressure of 253.3 kPa and with an Amberlyst 15 catalyst loading of $1.4 \text{ kg}_{\text{cat}}/\text{kg}_{\text{liquid}}$. These values were obtained or calculated from previous RD studies [10]. This pressure is necessary to achieve reasonably high temperatures for the reaction to proceed within the reactive stages. The H/V value, which is related to the distillation policy and the liquid hold-up in the reactive stages, was allowed to range from a distillation-controlled to a kinetically-controlled regime (0–1000 s). This range was calculate taking into account experimental data reported for a RD column in the synthesis of TEC [10]. The

obtained RRCM for different H/V values are presented in Fig. 3 using the reduced composition scales. It should be pointed out that such maps provides qualitative rather than quantitative information. They are introduced to understand the relative effect of varying the H/V value for different starting compositions.

As observed in the reactive residue curves from Fig. 2, an EtOH-rich mixture (near to the EtOH-H₂O azeotrope) can be obtained as distillate in direct sequences, while a mixture mainly composed of esters and CA would be the bottom product in indirect separations. According to the maps, the greater the H/V value, the greater the residence time inside a hypothetical reactive column. This explains why most of the reactive residue curves obtained at high H/V values have higher substitution degree (0.5–1), shifting the bottom

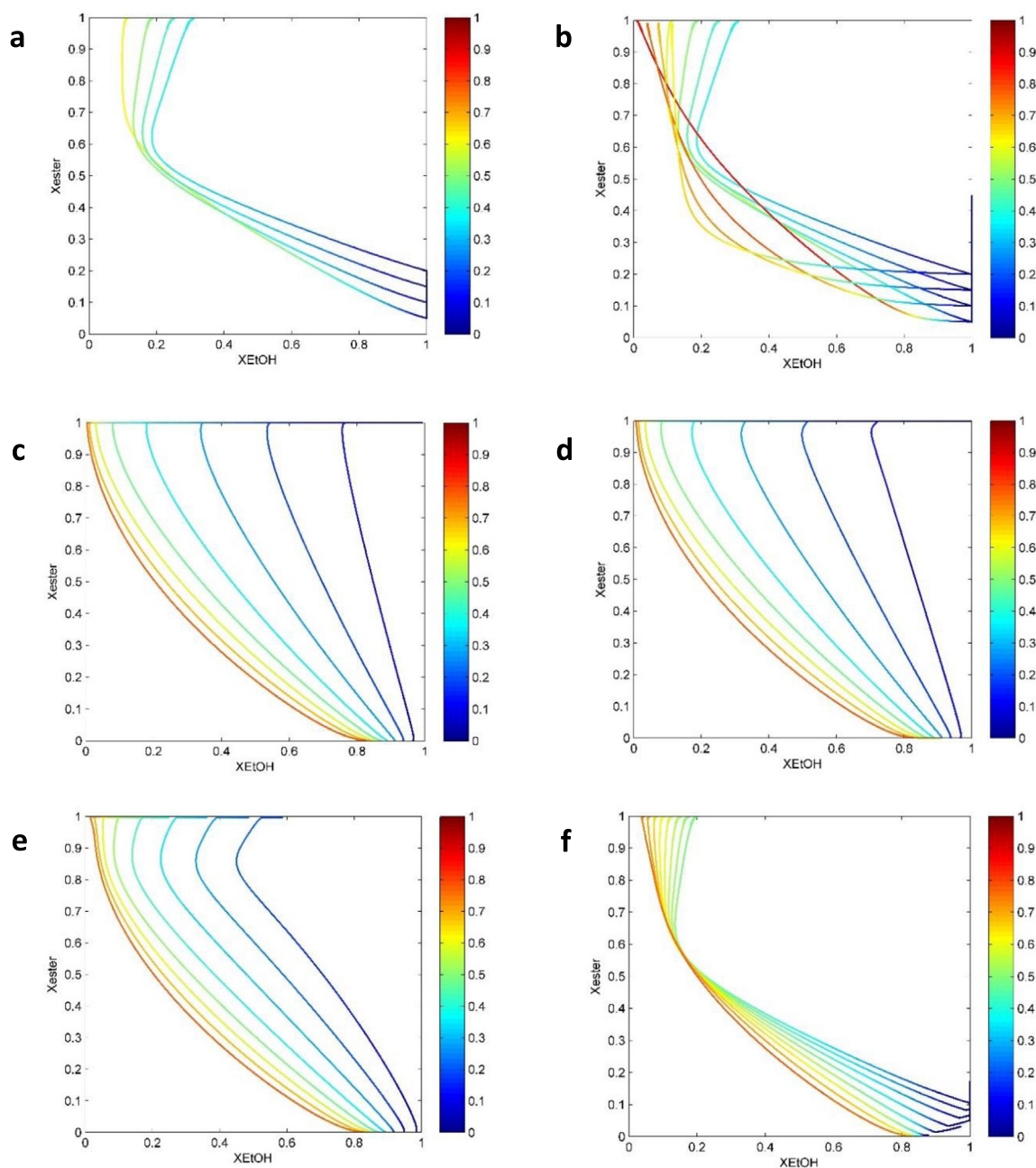


Fig. 2. Reactive residue curve maps for esterification of citric acid with ethanol. Color scale represents the substitution degree. Initial binary mixtures of pure ethanol and citric acid for a) H/V = 100 s; b) H/V = 1000 s. Initial multicomponent mixtures obtained with a batch pre-reactor for c) H/V = 0.1 s; d) H/V = 1 s; e) H/V = 10 s; f) H/V = 100 s. (For interpretation of the references to colour in this figure legend, the reader is referred to the web version of this article.)

product toward citric esters. The incomplete substitution observed in some curves indicates that kinetic reactions are slow and that

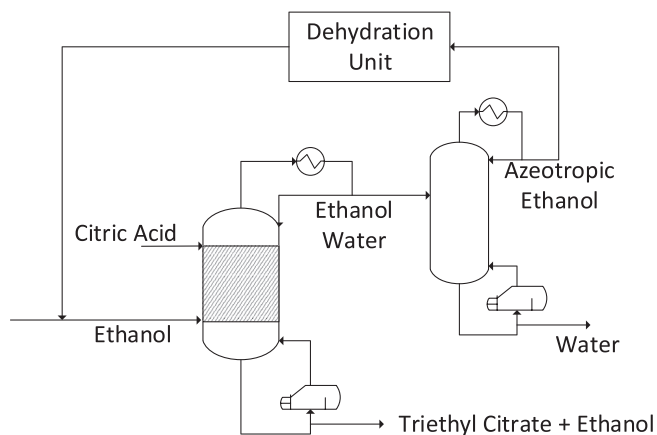


Fig. 3. Reactive distillation scheme for TEC production. Dashed area indicates reactive section.

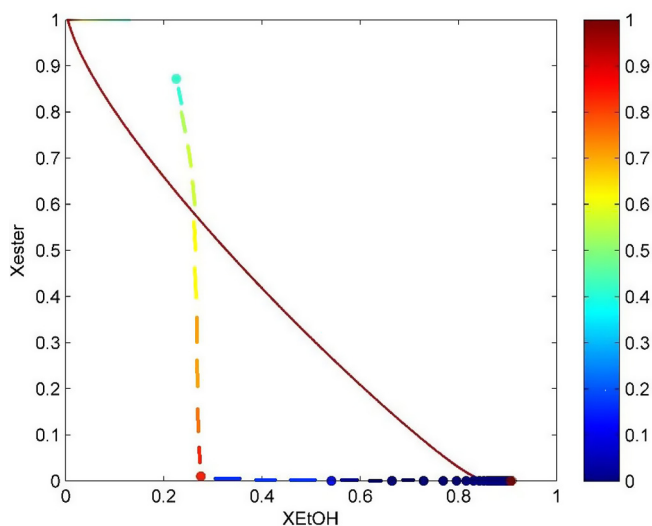


Fig. 4. Reactive residue curve for $H/V = 83.2$ s (continuous line), and simulated stage compositions for the reactive distillation base case (dash line with dots).

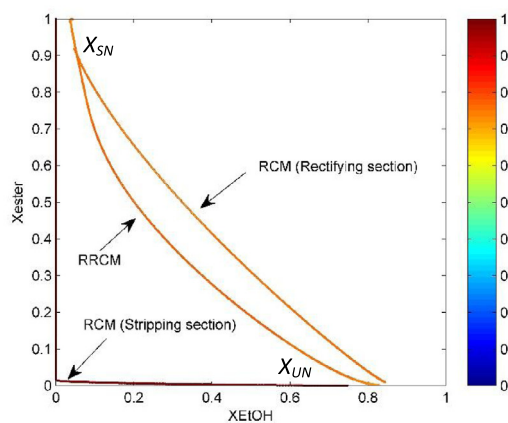


Fig. 5. Representation of a reactive dividing wall column using reactive and non-reactive residue curves for the hypothetical different sections. The color scale represents the substitution degree of citric acid. (For interpretation of the references to colour in this figure legend, the reader is referred to the web version of this article.)

longer residence times in the reactive stages are required. This seems to suggest that the use of significant excess of EtOH, and the potential need for side reactors instead of traditional catalytic internals is highly recommended.

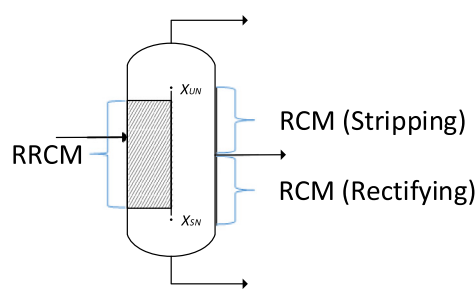
Even though high H/V values favor the reaction progress, extremely high values of H/V drive the reaction to chemical equilibrium and distillation is not efficiently accomplished. Since water is not completely distilled off, chemical equilibrium conversion is actually lower than the one achieved for intermediate values of H/V . This fact predicts the success of RD technologies for production of TEC, and suggests the need for non-reactive sections towards the top and bottom of the column.

According to the RRCM in Fig. 2, a RD column for TEC production will operate with a bottoms composition close to the stable node (citrate species) and a distillate composition close to the unstable node (EtOH-H₂O mixture). If the latter remains below the azeotropic molar fraction, the mentioned EtOH-H₂O stream may be further distilled to obtain azeotropic or anhydrous EtOH to be recycled. Based upon the RRCM analysis, a complete conceptual design of the RD operation is presented in Fig. 3.

To validate the feasibility of the obtained scheme, the RD column in Fig. 3 was simulated with a vast number of reactive stages (300), a large reflux ratio (600), and an oversized boilup ratio (5200). These conditions tried to represent the infinite number of stages and the infinite reflux assumptions applied in the RRCM construction. The composition profile of this RD column was contrasted with the equivalent reactive residue curve calculated with an H/V value of 83.2 s (experimental value calculated from [10]), and with an initial concentration corresponding to the chemical equilibrium composition of a feed ratio of EtOH:CA of 4:1 (Fig. 4). As observed, the RRCM does not match exactly the RD composition profile, which can occur for two reasons: first, a chemical equilibrium condition is achieved inside the simulated column due to the nearly infinite residence time; and second, the buildup of the highly volatile species (EtOH and water) inside the stages of the simulated column with extremely high reflux and boilup ratios. Despite the differences between both composition profiles, the predicted stable and unstable nodes lay closer to the top and bottom products composition of the column.

2.3. Conceptual design of the reactive dividing wall column

In order to predict the behavior of a reactive dividing wall column (RDWC) for TEC production, a similar approach to the one used before was implemented. In this case, it was assumed that



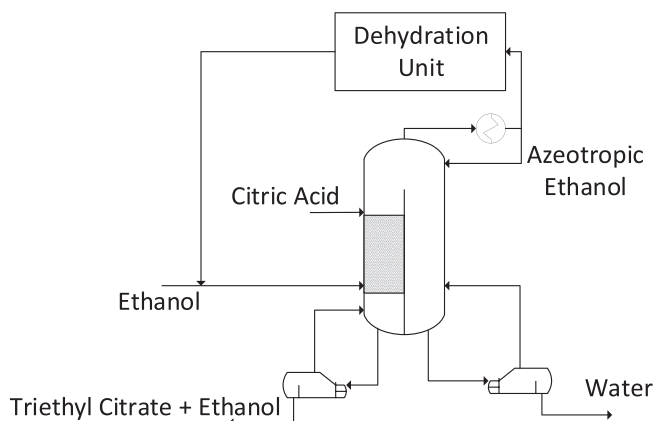


Fig. 6. RDWC scheme for TEC production. Dashed area indicates reactive section.

Table 2
Initial values for the main design variables in the base simulation for RD and RDWC schemes.

Variable	Nomenclature	RD	RDWC
EtOH feed stream (kg/h)	F_E	2260	2996
CA feed stream 50%wt (kg/h)	F_A	1806	1806
Heat duty – reactive column (kW)	Q_{1RD}	707	
Heat duty – prefractionator (kW)	Q_{1RDWC}		635
Heat duty – recovery column (kW)	Q_{2RD}	1000	
Heat duty – main column (kW)	Q_{2RDWC}		980
Reflux ratio reactive column (molar)	R_1	0.01	
Reflux ratio main column (molar)	R		2.3
Reflux ratio recovery column (molar)	R_2	0.2	–
Number of stages reactive column (main)	N_{F1}	120	120
Number stages recovery column	N_{RC}	14	–
Number of reactive stages	N_R	116	93
Feed stage EtOH	N_{FE}	118	91
Feed stage reactive mixture	N_{FA}	2	6
Liquid interconnection stream (kmol/h)	F_L		0.372
Column Diameter (m)	D	2.23	2.23
W _{cat} /stage (kg)	W_{cat}	17.8	17.8
Initial Reactive Stage	N_{FR}	3	7
Number of stages above wall	N_a	–	5

only one side of the dividing column contains catalyst, while the other was non-reactive. Using the RRCM compositions from Fig. 4, a vapor composition close to the unstable node (X_{UN}) and a liquid composition close to the stable node (X_{SN}) were selected. These two points represent the first stage just above and below the dividing wall, and they were used as the new starting compositions to calculate the traditional non-reactive residue curve trajectories (RCM). This was done by solving Eq. (17) from $\xi = 0$ to $\xi = \infty$ with initial concentration X_{UN} for the stripping section, and Eq. (18) from $\sigma = -\infty$ to $\sigma = 0$ with initial concentration X_{SN} for the rectifying section.

$$\frac{dx_i}{d\xi} = [x_i - y_i] \quad (17)$$

$$\frac{dx_i}{d\sigma} = -[x_i - y_i] \quad (18)$$

Fig. 5 presents the trajectories of the RRCM together with both RCM generated from X_{UN} and X_{SN} . As observed, the stable and unstable nodes from RRCM and RCM lines are the same since they belong to the same distillation region, however the trajectories are different as expected from the composition profiles at each side of the dividing wall.

Analyzing the RCM behavior for the stripping section, it is found that even though the SD value is very close to unity, the citrate

species content is very low ($X_{ester} \approx 0$, $X_{CA} \approx 0$). This is possible since the SD value only measures the degree of substitution of the citrate species, and not their amount. Therefore the composition of the saddle point is mainly water. This may suggest the utilization of a dividing wall near the unstable node (close to the EtOH-H₂O azeotrope) to obtain an additional product of high purity from the RDWC unit. On the other hand, the rectifying section shows a minor difference with respect to the RRCM which suggests that the utilization of a dividing wall near the stable node is not necessary. As a result of this preliminary analysis, a RDWC is expected to reduce the amount of equipment in the process and consequently the fixed costs. In Fig. 6 the proposed configuration for a RDWC is presented. This configuration avoids the use of an azeotropic unit while still obtaining the same product quality.

It should be pointed out that, despite it seems feasible in RRCM analysis, the bottom product of a RD column or a RDWC cannot be pure TEC. It is necessary to obtain the bottom product as a TEC-EtOH mixture in order to reduce the bubble temperatures in the reboiler. This would not only prevent from excessive decomposition of citrate species but also would avoid catalyst damaging. Taking this into account, a design specification was established to maintain the temperature below 423 K at any point within the column at the corresponding operating pressure.

2.4. Base cases implementation

Following the described processing schemes from Figs. 3 and 6, the steady state simulations of the base case scenarios of both RD and RDWC schemes were implemented in Aspen Plus 8.6[®]. The validated thermodynamic and kinetic models previously described were used during simulations, introducing the kinetic equation as a FORTRAN subroutine. Hydraulics of reactive and non-reactive sections were simulated using standard kerapak packing. A TEC production capacity of 10 kTon/yr, with a temperature limit of 423 K (i.e. TEC is diluted in ethanol to avoid decomposition of citrate species), and an operating pressure of 253.3 kPa were used as process specifications. Table 2 contains the values of the design parameters used to perform the preliminary simulations of the RD and RDWC schemes. The variables for the reactive column in the RD simulation were obtained from the plant-scale simulations presented by Kolah et al. [10]. The variables for the recovery column in the RD simulation were obtained from a Winn-Underwood-Gilliam method included in Aspen Plus: Reflux Ratio of 1.5 times the minimum, ethanol recovery of 99% (to minimize ethanol loss in the water stream), and water corresponding to the azeotropic concentration on the top. The RDWC base simulation was obtained from expanding the RD case and performing a sensitivity analysis over the main design parameters. Since the purpose of this work is to include controllability together with profitability at the early design stages, the benefit of having a base simulation is to reduce computational effort during the simultaneous optimization of both objective functions. Therefore, the traditional approach [28] of achieving a profitable design optimum first in order to carry out a subsequent controllability optimization is not necessary. The optimization of the design variables and operating variables is described in the next section.

3. Optimization of the proposed schemes

3.1. Optimization function

The combined functions used for the simultaneous optimization of RD and RDWC schemes, taking into account a profitability objective function (POF) and a controllability objective function (COF), are described in Eqs. (19) and (20) respectively.

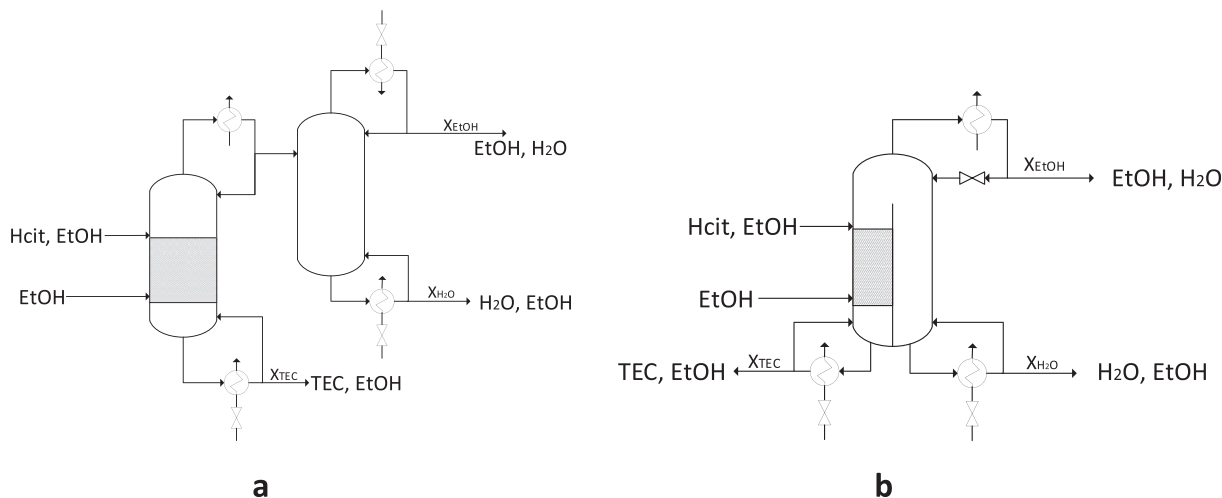


Fig. 7. Control structure for a) RD and b) RDWC.

$$\text{Min}(COF, POF)_{RD} = f(R_1, R_2, F_E, N_{T1}, N_{FA}, N_{FE}, W_C, N_{FR}, N_{R-RD}, Q_{1RD}, Q_{2RD}) \quad (19)$$

$$\text{Min}(COF, POF)_{RDWC} = f(R, F_E, F_L, N_{T1}, N_{FA}, N_{FE}, W_C, N_{FR}, N_{R-RDWC}, N_a, N_b, Q_{1RDWC}, Q_{2RDWC}) \quad (20)$$

The optimization functions are constrained by the maximum operating temperature and the desired purity of product streams according to Eqs. (21) and (22)

$$\bar{y}_i \geq \bar{x}_i \quad (21)$$

$$T_{\text{Reboiler}} \leq T_{\text{max}} \quad (22)$$

where y_i is the calculated mole purity and x_i is the desired purity of component i .

3.2. Controllability evaluation

In order to evaluate controllability, the control strategy presented in Fig. 7 was established according to traditional control heuristics [29]. Given the computational effort of solving the complete set of differential equations from a rigorous dynamic model along the optimization procedure, the dynamic model was approximated to a first order response [30]. This means each disturbance “ q ” in the manipulated variables will generate a response in the controlled variables “ p ” which can be approximated by an expression like Eq. (23), where k_{pq} and τ_q represents the gain and the characteristic time.

$$g(s) = \frac{k_{pq}}{1 + \tau_q s} \quad (23)$$

Therefore, a first order approximation requires less computational effort and time. Since there are three controlled variables together with three manipulated variables as shown in Table 3, the four steady state simulations represented in Fig. S.2 of the Supporting material, were carried out to obtain the entire 3×3 transfer matrix.

A sensitivity analysis over the base case was performed to select the disturbance constant of the manipulated variables. This was done to keep a convergence time below 10 s after the disturbance, while efficiently quantifying the gain from the controlled variables. A value of 0.3% was found as suitable disturbance constant, and it turned out to be similar to that suggested in previous reports [31].

Table 3
Controlled and manipulated variables for each intensified scheme.

Controlled Variable	Manipulated Variables	
	RD	RDWC
X_{EtOH}	R_1	R
X_{H_2O}	Q_{2RD}	Q_{2RDWC}
X_{TEC}	Q_{1RD}	Q_{1RDWC}

To calculate the gain matrix of each individual, the simulations for RD and RDWC were solved for the four steady state conditions mentioned above. According to the symbols of Fig. S.2, the first one is the undisturbed point (SS) and the other three (D1, D2 and D3) have a 0.3% disturbance in the manipulated variable (MV) value. The time constant (τ_q) after every perturbation was calculated following the methodology proposed by Skogestad & Morari [28] using Eqs. (24) and (25).

$$\tau_q = \frac{\text{change in holdup of one component (kmol)}}{\text{imbalance in supply of this component } \left(\frac{\text{kmol}}{\text{min}}\right)} = \frac{\sum_{f=1}^{N+1} M_f \Delta x_i}{\Delta S_i} \quad (24)$$

$$\Delta S_i = |D_{f1} y_{D1} - D_{f0} y_{D0}| + |B_{f1} x_{B1} - B_{f0} x_{B0}| \quad (25)$$

Here, D_f and B_f correspond to the molar flow of distillate and bottoms product streams respectively; x_B and y_D correspond to the mole fraction of the analyzed component in each product stream; M_f corresponds to the molar holdup of stage f ; and ΔS_i is the supply imbalance of component i due to a given disturbance. The subscripts 0 and 1 indicate the initial and final stable state condition before and after the perturbation was carried out.

To evaluate the controllability of a given individual (i. e. a processing scheme under certain operating conditions), a singular value decomposition (SVD) analysis was carried out from the gain matrix of the process. To do this, the transfer matrix was transformed from the Laplace to the frequency domain ($s = \omega i$) according to Eq. (26).

$$g(s) = g(\omega i) = \frac{k_{pq}(1 - \tau_q \omega i)}{1 + \tau_q^2 \omega^2} \quad (26)$$

Finally, the condition number was calculated according to Eq. (27). In order to evaluate the controllability in the frequency range from 0 to 1000 as suggested by Cabrera-Ruiz et al. [20], the area

under the curve of condition number against frequency (see Fig. S.3 in Supplementary material) was considered as the COF (Eq. (28)). This methodology has been discussed in detail and successfully applied in the controllability analysis of similar studies [21]. The COF values for the RD and RDWC base simulations are 7.3×10^5 and 1.1×10^6 respectively. It should be pointed out that the condition number and hence the COF are not absolute values since they depend on the controlled and manipulated variable units. Therefore, they are only comparable among equivalent simulations like the ones presents in this work.

$$\text{Condition Number (CN)} = \frac{\text{Minimum Singular Value } (\sigma_{\min})}{\text{Maximum Singular Value } (\sigma_{\max})} \quad (27)$$

$$\text{COF} = \int_0^{1000} \text{CN} dw \quad (28)$$

3.3. Cost evaluation

The profitability objective function (POF) was calculated using the total annual costs (TAC) of each configuration according with Eq. (29).

$$\text{POF} = \text{TAC} = \text{capital costs} + \text{Operating costs} \quad (29)$$

Guthrie's correlations were used to estimate the capital costs [29,32], including the catalyst price within the cost of the column. Since the column structured packing is not included in Guthrie's correlations, the annual operating cost mentioned by Niesbach et al. was used to predict the structured packing cost contribution [33]. For the RD and RC units, the diameter was calculated from Aspen simulations through the pack sizing tool assuming Kerapack type structure. The same strategy was used to calculate the diameter of the prefractionator (D_{prefac}^2) and main (D_{main}^2) sections in the RDWC case in order to use Eq. (30) to estimate an equivalent diameter for the cost calculation. Stainless steel was selected as construction material for RDWC and RD while carbon steel was used for the RC as no acid species were found to exit the distillate from the RD column. A height per stage of 0.6 m was used to calculate the column total height. The updated prices for raw materials, products and utilities were used in the calculation of operating costs. A three year for return on investment was used for a production facility of 10 kTon/yr as suggested by our industrial partner.

$$D_e = \sqrt{D_{\text{prefac}}^2 + D_{\text{main}}^2} \quad (30)$$

3.4. Optimization method

The optimization of both intensified configurations for TEC production was carried out with a multi-objective differential evolution method (MODE) together with a tabu list algorithm, as

proposed by Sharma and Rangaiah [34]. The flowchart algorithm for the optimization process is presented in Fig. S.4 in the Supplementary material. Initially, a population of $2 \times \text{NP}$ individuals (NP is the population size) is randomly generated within the bounds of the decision variables, and both objective functions (COF and POF) are evaluated. Best individuals within the population are the first parents, and worst individuals are the first tabu population. From this point on, the algorithm is executed for the maximum number of generations (MNG) according to the following procedure: trial individuals are generated from the last set of parents using mutation (Pm) and crossover (Pc) probability, making sure they do not come closer than the tabu radius to any individual from the tabu list. Both objective functions are evaluated for the trial individuals, and non-dominated sorting is carried out to obtain mutually-exclusive-non-dominated sets or fronts, using the trial individuals and the last set of parents. Then, fronts are organized by rank and accepted into the child population in descending order until the number of individuals exceeds NP. Crowding distance calculation is performed to select the individuals with the largest crowding distance from the last front to complete a child generation of exactly NP individuals. Individuals which were not accepted into the child population make part of the updated tabu list, and the child generation will become the new generation of parents. This optimization tool was programmed as a Visual Basic Macro within Excel.

This optimization method has been previously found successful in solving similar multi-objective problems from the chemical engineering industry [31]. In Table 4 it is summarized the set of parameters used during optimization. The values for cross over and mutation probability were selected according with the original report describing the applied optimization method [34].

Table 5
Optimization variables and ranges for the RD and RDWC schemes.

Variable	RD scheme		RDWC scheme	
	Min	Max	Min	Max
F_E (kg/h)	1382	3686	1152	3686
Q_{1RD} (kW)	550	900		
Q_{2RD} (kW)	500	1320		
Q_{1RDWC} (kW)			550	800
Q_{2RDWC} (kW)			300	1500
R_1	0.001	1	0.7	3.0
R_2	0.5	3.5		
N_{TI}	60	130	70	120
N_R	60	128	50	118
N_{FE}	1	25	1	10
N_{FA}	2	10	1	10
F_L (kmol/h)			0.005	1.5
W_C (kg cat /stage)	3.5	32.2	3.5	32.2
N_{FR}	2	10	1	10
N_b			1	15
$N_b - N_a$			10	115

Table 4
Parameters for the MODE.

Parameter	Value
Number of Objective Functions	2
Number of Optimization Variables	11–13
Cross Over Probability	0.3
Mutation Probability	0.5
Tabu List	100
Tabu radius	0.0000025
Population Size	200
Number Generations	200
Temperature Constrain	423 K
Water mole purity constrain	0.9
EtOH mole purity constrain	0.85

Table 6
List of models and tools used during optimization procedure.

Section	Equations	Software
Thermodynamics	UNIQUAC model	Aspen
Kinetics	1–7	Fortran/Aspen
Optimization Algorithm	19–22	VBA
Steady state simulation	Radfrac model	Aspen Plus 8.6
Controllability evaluation (COF)	23–28	Matlab
Profitability evaluation (POF)	29 (Guthrie's correlations)	Excel Spreadsheet

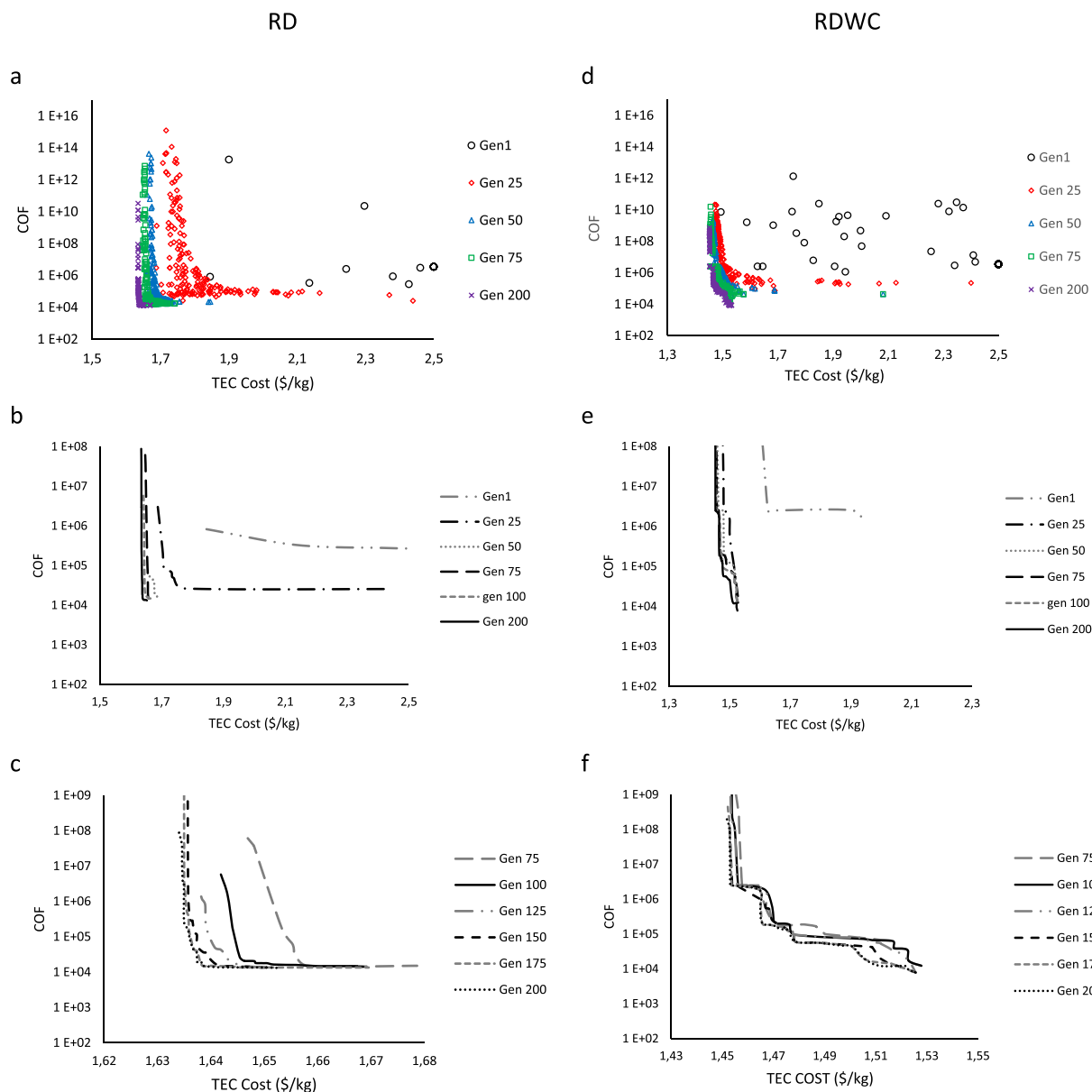


Fig. 8. Best 200 individuals (Parents) along evolution for a) RD and d) RDWC. Pareto Front displacement along evolution for b) RD and e) RDW. Plots c) and f) are magnifications of the optimal zones of RD and RDW configurations, respectively.

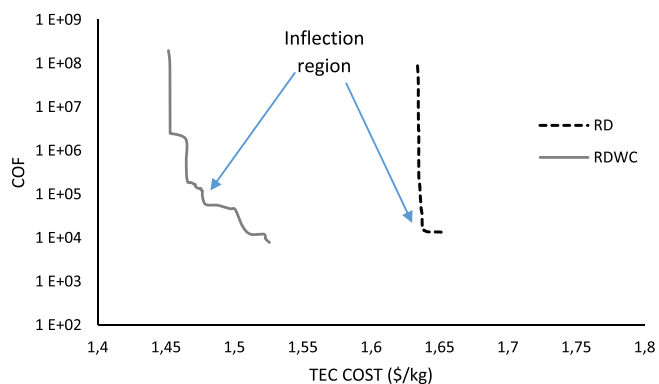


Fig. 9. Final Pareto fronts for the multi-objective optimization of TEC production by using RD and RDWC schemes.

A preliminary sensitivity analysis was performed for both base cases to identify suitable ranges of variation for the design vari-

ables, and to assure that the generated individuals were possible solutions. Nevertheless this does not guarantee convergence when all optimization variables are allowed to vary. The algorithm was then executed 20 times for 5 generations to discard that the Pareto front was being limited by a given variable range. Optimization variable bounds were adjusted accordingly. Final ranges are presented in Table 5 for RD and RDWC, respectively. Table 6 presents a model summary for the different types of software and equations used in each optimization section.

4. Results and discussion

The optimization procedure for each configuration lasted around 200 h, using a computer with a core-i7 processor and 3 Gb DDR. The evolution of objective functions and the first non-dominated solution set, with the increase in the number of generations is presented in Fig. 8 for both, RD and RWDC optimization results. The controllability objective function (COF) and the

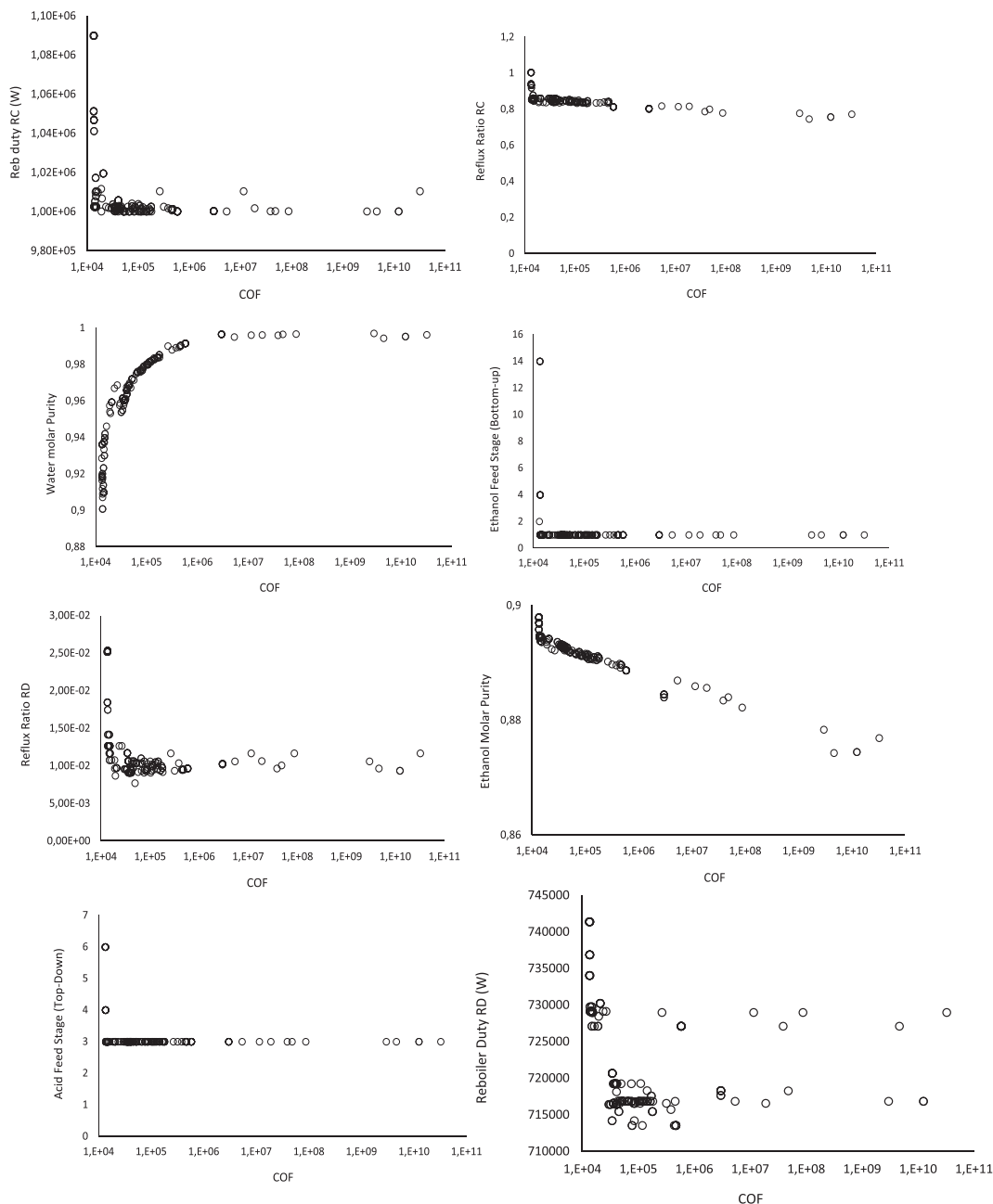


Fig. 10. Design variables, operational variables and resulting purities dependence with COF for the RD scheme.

calculated cost per kilogram of TEC (obtained from total costs and production rate) were tracked during the optimization process. Fig. 8a and d show how the parent sets come closer to the first non-dominated set or Pareto front as the algorithm evolves. Fig. 8b, c, e and f show the displacement of the Pareto front with the increase in the generation number. It can be seen that ca. 125 generations are enough to achieve an optimal front. Beyond this point less than 1% variation in the Pareto front is observed indicating the algorithm is coming closer to a global optimum front. Fig. 8 also shows the clear competition between the two optimization functions.

The final Pareto front after 200 generations for RD and RDWC is presented in Fig. 9. As before, this plot includes TEC production costs instead of TAC, to provide a more meaningful numeric result. In order to decide the desirable operating conditions for the RD or the RDWC scheme, a compromise between acceptable costs and an

easily controllable technology must be established. From Fig. 9 it can also be noticed that the RDWC scheme exhibits 7–11% cost savings over the RD system. This is important taking into account that raw materials represent the highest cost in TEC production. It is therefore reasonable to think that this improvement will impact the competitiveness of TEC in the plasticizers market.

Regarding controllability, there is no significant difference in the COF between the RDWC and the RD scheme, indicating both alternatives have similar controllability properties. This behavior is surprising since any perturbation in the RDWC system would affect the purity of the three product streams. In contrast, in the RD scheme, disturbances in the recovery column do not affect the reactive unit performance. Furthermore, the material and energy integration within the RDWC system reduces its operability window, and it was expected to have a negative impact on controllability. Figs. 10 and 11 present the tendencies of the optimization

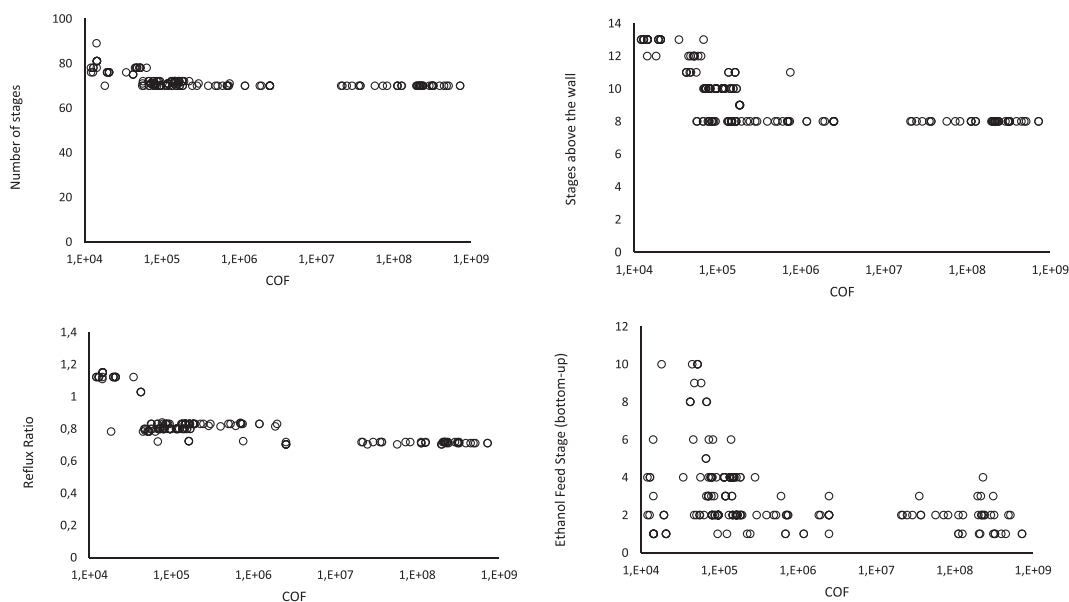


Fig. 11. Design variables, operational variables and resulting purities dependence with COF for the RDWC scheme.

Table 7
Optimization results of the inflection point in Fig. 9.

Variable	RD	RDWC
EtOH stream (kg/h)	1771	1637
CA stream (kg/h)	1801	1812
Heating duty column 1 (pre fractionator) (kW)	717	710
Heating duty column 2 (kW)	998	366
Reflux ratio column 1 (pre fractionator)	0.01	0.80
Reflux ratio column 2	0.86	–
TEC (kg/h)	1291	1291
Number of stages column 1 (pre fractionator)	60	70
Number stages column 2	20	38
Number of reactive stages	57	56
Conversion of CA (%)	100	100
Selectivity to TEC (%)	99.7	99.1
Energy consumption (kJ/kg TEC)	4780	3003

variables with respect to the COF for the optimal pareto set of the RD and RDWC schemes respectively. Bearing in mind that COF and POF are competing goals the following may be interpreted for the design variables, operational variables and resulting purities.

In the RD case, the lower the acid feed stage and the upper the ethanol feed stage, there are more stages for stripping and rectifying and therefore more controllability. Additionally, more stages account for bigger columns which also explains the cost increase. Operational variables like reflux ratio of RC and RD have been found to increase controllability since they increase the separation efficiency while increasing reboiler duty and therefore operational cost. The more controllable conditions result in lower water purities and therefore lower EtOH recovery which in place increases the TAC.

In the RDWC case, a similar effect is observed regarding the design variables. Those variables accounting for bigger columns like total number of stages, EtOH feed stage or number of stages above the wall, imply higher costs and better controllability. Regarding the operational variables, high reflux ratios result in higher costs and better controllability. It is interesting to note that in the RDWC there are less variables that have a direct relation with the optimization variables. This is due to the complexity and non-linearity of the models that describe the system and therefore the complexity of the optimization problem.

Additional closed loop dynamic simulations were carried out in Aspen Dynamics 8.6[®] with a sample of 5 individuals from the final Pareto fronts. It was found that both schemes are able to support step perturbations from 1 to 10% of the manipulated variables while maintaining the operation under control. Table 7 presents the results of the main design and operating variables for simulations located in the inflection zone of Fig. 9, and that therefore may be selected as the preferable solutions from the Pareto front. From these results, the RDWC has been found to be less energy and material intensive for the same TEC productivity. For this scheme, there is a consumption increase in CA (ca. 1%), a reduction in EtOH use (ca. 8%) together with energy savings of 37%. These results agree with most reports regarding the benefits obtained by using dividing wall columns [17,35–37] and are particularly interesting as processing costs are becoming more important as we move from conventional to renewable energy sources [38]. With respect to selectivity, we can observe that even though both alternatives have a CA conversion of 100%, neither can achieve 100% selectivity towards TEC mainly due to unconverted DEC. This intermediate ester exits the columns from the bottoms of the reactive unit together with TEC and some EtOH. This was previously observed in pilot scale experiments operating near atmospheric pressure [10]. This indicates that a RDWC with the use of pre-reactor or/and the use of side reactors at higher pressure, would be a suitable intensified system to achieve a complete conversion to TEC.

The composition profiles along the columns from both schemes under optimal conditions are presented in Fig. 12. Under these conditions, DEE production is negligible in both schemes. As expected from the previous analysis, the composition profile of the reactive side of the RDWC is very similar to the RD one, while the other side is used to obtain pure water from the bottoms.

5. Conclusions

Two different intensified configurations for the production of triethyl citrate have been developed, a reactive distillation system and a reactive dividing wall column system. Reactive residue curve maps were used to establish the feasibility of both configurations, and to obtain preliminary information needed for processes modeling. Rigorous simulations of both alternatives were carried out,

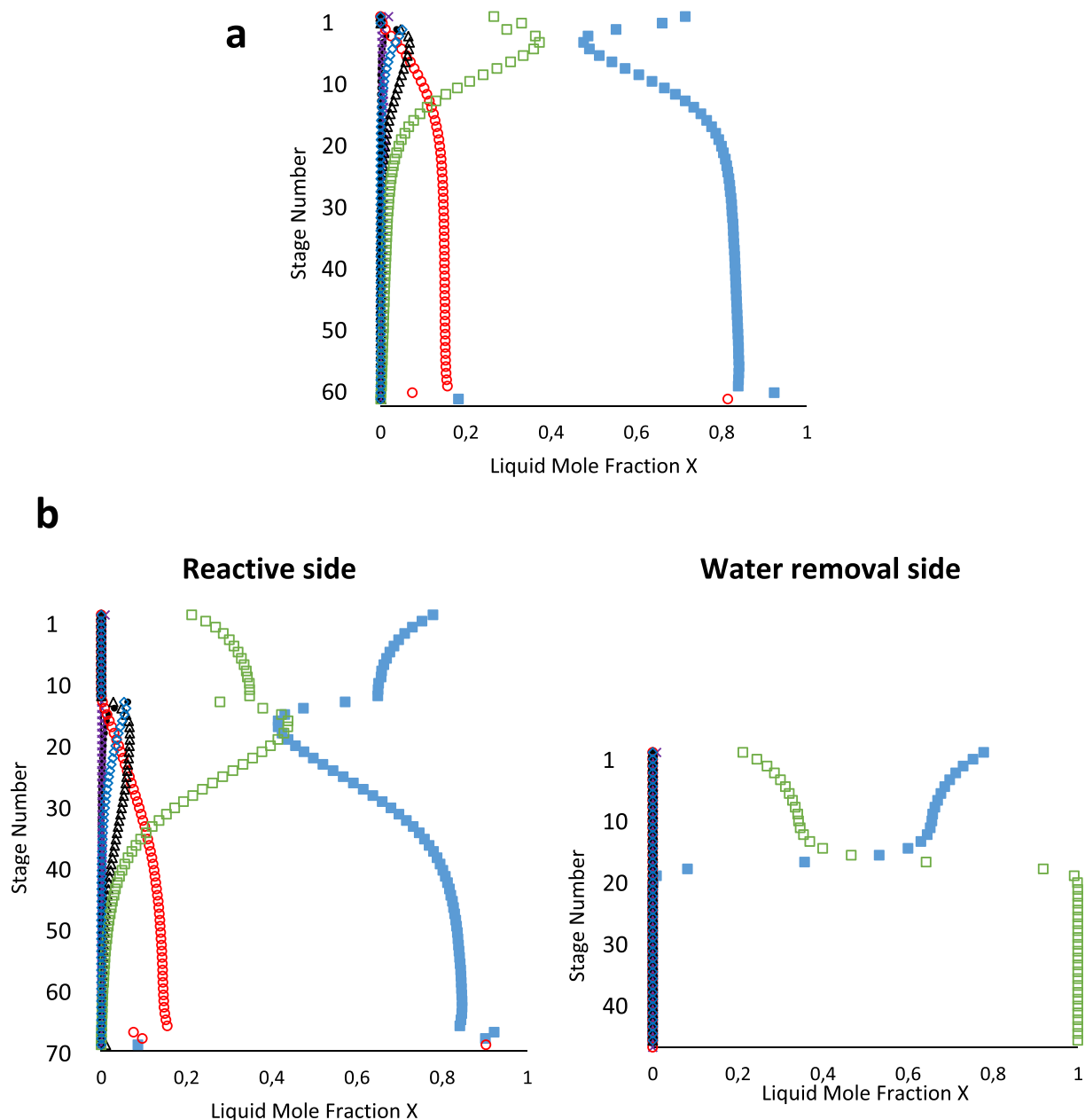


Fig. 12. Composition profile in reactive distillation schemes a) RD and b) RDWC. (●) CA; (■) EtOH; (◇) MEC; (△) DEC; (○) TEC; (□) H₂O; (×) DEE.

and further used in a multiobjective optimization problem. The condition number integral in the frequency range was used as the controllability objective function, and the total annual costs was used as the profitability objective function. Over 40,000 individuals were evaluated for each production scheme, and results show conflict between costs and controllability goals. Regarding controllability, both schemes offer similar properties. Additionally the RDWC alternative offers ca. 11% savings in TAC costs over RD, and energy savings of around 40%. The novel methodology proposed for the design of a TEC production via intensified processes was found to be successful.

Acknowledgements

This work is supported by Colombian Administrative Department of Science, Technology and Innovation (COLCIENCIAS) under the project: “Producción de plastificantes a partir de ácido cítrico

usando procesos híbridos de reacción y separación simultánea” cod. 1101-569-33201. Miguel Santaella acknowledges the research group at Universidad de Guanajuato for their accompaniment, sharing and support during his visit to Guanajuato.

Appendix A. Supplementary data

Supplementary data associated with this article can be found, in the online version, at <http://dx.doi.org/10.1016/j.cej.2017.07.015>.

References

- [1] C. Emanuel, Plasticizers market update, in: 22nd Annual Vinyl Compounding Conference, BASF The Chemical Company, Burlington, 2011.
- [2] S.N. Bizzari, M. Blagoev, A. Kishi, Plasticizers, in: Chem. Econ. Handb., Online Edi, SRI Consulting, Menlo Park, CA, 2015, p. 148.
- [3] L.G. Krauskopf, How about alternatives to phthalate plasticizers?, J Vinyl Addit. Technol. 9 (2003) 159–171, <http://dx.doi.org/10.1002/vnl.10079>.

- [4] W.D. Arendt, M. Joshi, Specialty plasticizers, in: Richard F. Grossman (Ed.), *Handb. Vinyl Formul., Second ed.*, John Wiley & Sons, Inc, 2008, pp. 239–286.
- [5] M. Rahman, C. Brazel, The plasticizer market: an assessment of traditional plasticizers and research trends to meet new challenges, *Prog. Polym. Sci.* 29 (2004) 1223–1248, <http://dx.doi.org/10.1016/j.progpolymsci.2004.10.001>.
- [6] M. Johnson, Final report on the safety assessment of acetyl triethyl citrate, acetyl tributyl citrate, acetyl trihexyl citrate, and acetyl trioctyl citrate 1, *Int. J. Toxicol.* 21 (2002) 1–17, <http://dx.doi.org/10.1080/1091581029009650>.
- [7] J. García-Serna, L. Pérez-Barrigón, M.J. Cocero, New trends for design towards sustainability in chemical engineering: green engineering, *Chem. Eng. J.* 133 (2007) 7–30, <http://dx.doi.org/10.1016/j.cej.2007.02.028>.
- [8] A.A. Upahye, W. Qi, G.W. Huber, Conceptual process design: a systematic method to evaluate and develop renewable energy technologies, *Aiche J.* 57 (2011) 2292–2301, <http://dx.doi.org/10.1002/aic>.
- [9] A.K. Kolah, N.S. Asthana, D.T. Vu, C.T. Lira, D.J. Miller, Reaction kinetics of the catalytic esterification of citric acid with ethanol, *Ind. Eng. Chem. Res.* 46 (2007) 3180–3187, <http://dx.doi.org/10.1021/ie060828f>.
- [10] A.K. Kolah, N.S. Asthana, D.T. Vu, C.T. Lira, D.J. Miller, Triethyl citrate synthesis by reactive distillation, *Ind. Eng. Chem. Res.* 47 (2008) 1017–1025, <http://dx.doi.org/10.1021/ie070279t>.
- [11] D. Miller, N. Asthana, A. Kolah, D. Vu, C. Lira, Process for reactive distillation esterification, US Patent 7667068, 2010.
- [12] D. Sutton, G. Reed, A. Hiles, Process for the production of esters of mono-, di- or polycarboxylic acids, US Patent 7816554 B2, 2010.
- [13] A. Orjuela, C. Martinez, E. Molina, L. Jimenez, Optimization of a Reactive Distillation Process for Producing Triethyl Citrate, in: AIChE 2013 annual meeting, San Francisco, 2014.
- [14] C.B. Panchal, J.C. Prindle, A. Kolah, D.J. Miller, C.T. Lira, Integrated process of distillation with side reactors for synthesis of organic acid esters, US Patent 9174920 B1, 2015.
- [15] A. Kolah, C. Lira, D. Miller, R. Doctor, J. Prindle, C. Panchal, Heat Integrated Reactive Distillation Using External Side Reactors for Synthesis of Tri-Ethyl Citrate, in: AIChE Spring Meeting 2014, New Orleans, 2014.
- [16] M. Santaella, G. Rodriguez, A. Orjuela, Design of a thermally coupled reactive distillation sequence for triethyl citrate production, in: Aiche 2014 Annual Meeting, Atlanta GA, 2014.
- [17] Ö. Yildirim, A.A. Kiss, E.Y. Kenig, Dividing wall columns in chemical process industry: a review on current activities, *Sep. Purif. Technol.* 80 (2011) 403–417, <http://dx.doi.org/10.1016/j.seppur.2011.05.009>.
- [18] N. Sharma, Control of reactive distillation column: a review, *Int. J. Chem. React. Eng.* 8 (2010).
- [19] F.O. Barroso-muñoz, S. Hernández, B. Ogunnaike, Analysis of design and control of reactive thermally coupled distillation sequences, *Comput. Aided Process Eng.* 24 (2007) 877.
- [20] J. Cabrera-Ruiz, J.G. Segovia-Hernández, J.R. Alcántara-ávila, S. Hernández, Optimal dynamic controllability in compressor-aided distillation schemes using stochastic algorithms, *Comput. Aided Process Eng.* 30 (2012) 552–556.
- [21] C. Ramírez-Márquez, J. Cabrera-Ruiz, J.G. Segovia-Hernandez, S. Hernández, M. Errico, B.G. Rong, Dynamic behavior of the intensified alternative configurations for quaternary distillation, *Chem. Eng. Process. Process Intensif.* 108 (2016) 151–153.
- [22] C. Berdugo, A. Orjuela, M. Santaella, L.E. Plazas, A. Espinosa, Separation of Diethyl Citrate and Phase Equilibria in Mixtures with Ethanol and Water, in: *Sep. Div., Aiche Annual Meeting*, Salt Lake City, 2015.
- [23] A. Daneshfar, M. Baghlani, R.S. Sarabi, R. Sahraei, S. Abassi, H. Kaviyan, et al., Solubility of citric, malonic, and malic acids in different solvents from 303.2 to 333.2K, *Fluid Phase Equilib.* 313 (2012) 11–15, <http://dx.doi.org/10.1016/j.fluid.2011.09.033>.
- [24] D. Wyrzykowski, E. Hebanowska, G. Nowak-Wicz, M. Makowski, L. Chmurzyński, Thermal behaviour of citric acid and isomeric aconitic acids, *J. Therm. Anal. Calorim.* 104 (2011) 731–735, <http://dx.doi.org/10.1007/s10973-010-1015-2>.
- [25] M.M. Barbooti, D.A. Al-Sammerrai, Thermal decomposition of citric acid, *Thermochim. Acta.* 98 (1986) 119–126, [http://dx.doi.org/10.1016/0040-6031\(86\)87081-2](http://dx.doi.org/10.1016/0040-6031(86)87081-2).
- [26] C. Thiel, K. Sundmacher, U. Hoffmann, Synthesis of ETBE: Residue curve maps for the heterogeneously catalysed reactive distillation process, *Chem. Eng. J.* 66 (1997) 181–191, [http://dx.doi.org/10.1016/S1385-8947\(96\)03173-7](http://dx.doi.org/10.1016/S1385-8947(96)03173-7).
- [27] D. Barbosa, M. Doherty, The simple distillation of homogeneous reactive mixtures, *Chem. Eng. Sci.* 43 (1988) 541–550.
- [28] M. Asteasuain, C. Sarmoria, A. Brandolin, A. Bandoni, Integration of control aspects and uncertainty in the process design of polymerization reactors, *Chem. Eng. J.* 131 (2007) 135–144, <http://dx.doi.org/10.1016/j.cej.2006.12.029>.
- [29] W.D. Seider, J.D. Seader, D.R. Lewin, S. Widagdo, *Product and Process Design Principles: Synthesis Analysis and Evaluation*, John Wiley & Sons Inc, Hoboken, NJ, 2009.
- [30] S. Skogestad, M. Morari, The dominant time constant for distillation columns, *Comput. Chem. Eng.* 11 (1987) 607–617.
- [31] C.E. Torres-ortega, J.G. Segovia-hernández, F.I. Gómez-castro, S. Hernández, A. Bonilla-petriciolet, B. Rong, Design, optimization and controllability of an alternative process based on extractive distillation for an ethane – carbon dioxide mixture, *Chem. Eng. Process. Process Intensif.* 74 (2013) 55–68.
- [32] J.M. Douglas, *Douglas - Conceptual Design Of Chemical Processes*, McGraw-Hill, 1988.
- [33] A. Niesbach, H. Kuhlmann, T. Keller, P. Lutze, A. Górak, Optimisation of industrial-scale n-butyl acrylate production using reactive distillation, *Chem. Eng. Sci.* 100 (2013) 360–372, <http://dx.doi.org/10.1016/j.ces.2013.01.035>.
- [34] S. Sharma, G.P. Rangaiah, Modeling and optimization of a fermentation process integrated with cell recycling and pervaporation for multiple objectives, *Ind. Eng. Chem. Res.* 51 (2012) 5542–5551, <http://dx.doi.org/10.1021/ie202205h>.
- [35] A.A. Kiss, H. Pragt, C. Van Strien, Overcoming equilibrium limitations in reactive dividing-wall columns, *Comput. Aided Chem. Eng.* 24 (2007) 467–472.
- [36] A.A. Kiss, *Applications of dividing-wall columns*, *Adv. Distill. Technol. Des. Control Appl.*, John Wiley & Sons, Inc, Chichester, UK, 2013.
- [37] I. Mueller, E.Y. Kenig, Reactive distillation in a dividing wall column: rate-based modeling and simulation, *Ind. Eng. Chem. Res.* 46 (2007) 3709–3719, <http://dx.doi.org/10.1021/ie0610344>.
- [38] J.P. Lange, Lignocellulose conversion: an introduction to chemistry, process and economics, *Biofuels, Bioprod. Biorefin.* 1 (2007) 39–48, <http://dx.doi.org/10.1002/bbb>.